Strength Evaluation by Ultrasonic Methods

J. D. ACHENBACH
Center for Quality Engineering and Failure Prevention, Northwestern University, Evanston, IL. 60208, USA

ABSTRACT

Ultrasonic methods to detect and characterize cracks are discussed with a view towards the non-destructive determination of the reduction of strength due to the presence of flaws. The relation between quantitative ultrasonics and strength considerations is considered in some detail. Mathematical modelling for the direct problem of scattering of ultrasonic waves by cracks, as well as for the inverse problem of crack characterization from scattering data, is reviewed. For a problem of quasi-static loading, the Mode-I stress intensity factor induced by the presence of a crack, has been computed directly from the results of a related inverse scattering problem. The analytical work is based as the assumption of a perfect crack geometry. The effects of deviations from a perfect geometry due to near-tip zones of different mechanical properties, partial crack closure and the presence near the crack tips of discrete secondary scatterers such as microcracks, voids and inclusions, are also discussed.

KEYWORDS

Quantitative non-destructive evaluation, ultrasonics, crack characterization, stress intensity factors.

1. Introduction

Cracks in structural components are undesirable, and one can take the point of view that any component which contains a detectable crack should be rejected. Within the theoretical framework of the mechanics of fracture, this would, however, not be a productive point of view, because not all cracks are necessarily harmful over the service life of the component. A more effective approach is to detect and then characterize a crack by a non-destructive method, i.e., determine its location, size, shape and orientation. When the geometrical configuration of a crack is known, the maximum value of the stress intensity factor can be calculated, and the criticality of the crack can be assessed. An even more desirable result would be if a non-destructive test would yield direct information on the maximum value of the stress intensity factor for specified service loads, without the intermediate step of characterization of the crack geometry.

Both approaches, with the second being as yet unproven in practical applications, require sophisticated methods of quantitative non-destructive evaluation.

A single crack is only one kind of material discontinuity. Cracks are particularly objectionable since they are very obvious causes of catastrophic failure, but voids, cavities, inclusions, interfaces, distribution of cracks, or in general terms damaged regions of a material, may have equally deleterious effects on the strength of components. By the use of appropriate non-destructive evaluation methods it should be possible to discriminate between a broad spectrum of flaws and to determine the relevant characteristics of each kind. For purposes of specificity within the allotted length of this paper, the attention will, however, be restricted to components containing cracks.

Most methods of non-destructive evaluation provide only limited information. For strength evaluation it is, however, not good enough just to detect a flaw or the presence of inferior material properties. Quantitative information is required. This need has given rise to a more rigorous and fundamental approach to non-destructive evaluation which is called Quantitative NDE (QNDE).

Nondestructive evaluation (testing) methods include radiography, eddy current methods, dye penetrants, ultrasonic methods, optical methods, thermal wave imaging, x-ray and neutron scattering methods and methods based on nuclear magnetic resonance. Each method has its advantages and disadvantages for particular applications.

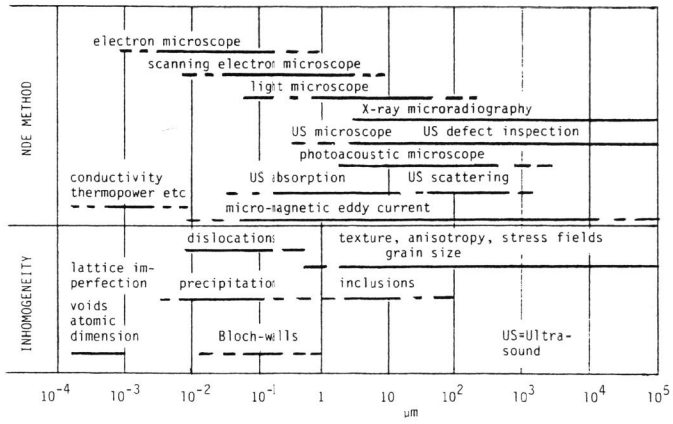

Fig. 1 Range of linear dimensions of material inhomogeneities, and examination methods, after Höller [1].

Some methods of quantitative non-destructive evaluation are laboratory methods, others are already being used extensively in the field. The distinction is primarily one of resolution of linear dimensions of micro-structural parameters. The smallest dimensions can be resolved only with sensitive laboratory equipment. On the other hand macrolevel cracks can be detected and characterized with robust equipment that can easily be transported and put in operation. Figure 1, after Höller [1], shows the range of linear dimensions of various material inhomogeneities in the lower part, while the upper part lists available examination methods. If we

restrict our attention to inhomogeneities with dimensions above one micron, then inclusions, grain sizes, texture, anisotropy and residual stresses cover more than four orders of magnitude of linear dimensions. It should be noted that ultrasonic resolutions has come down to microns by gigahertz ultrasonic microscopy. Ultrasonic scattering becomes effective slightly below 10 microns in materials with low absorption.

The great advantage of ultrasonic techniques is that they are relatively simple. Mechanical waves are used to penetrate a material and so mechanical properties and defects, that are most closely related to useful life and eventual failure, are measured directly. A considerable fraction of the research efforts in QNDE is, therefore, concerned with ultrasonic measurement techniques. This paper will consider only ultrasonic methods for quantitative non-destructive evaluation. The emphasis will be on bodies that contain one or more compact flaws, particularly cracks.

A compact flaw acts as a reflector of ultrasonic wave motion. A bigger flaw reflects more sound, and hence the amplitude of the voltage produced by a piezoelectric transducer that is exposed to the reflected sound is related to the dimensions of the crack. Unfortunately, quantitative characterization of a flaw based on amplitude measurements may be very inaccurate unless the measurement is carefully calibrated. The reason is that part of the incident energy that insonifies the flaw is scattered rather than specularly reflected. A calculation of the total fields which includes scattering effects is rather complicated. Another problem with amplitude considerations is that damping in the material and scattering by secondary sources, such as microstructure, microcracks, voids and inclusions, tend to reduce the measured signals, particularly as the frequency increases. Hence the productive use of amplitude considerations requires careful adjustment of the results for the effects mentioned above.

In an alternative approach it is attempted to characterize a flaw on the basis of measured travel times for signals which travel different paths, that are related to the geometrical configuration of the flaw. This time of flight approach, which is an application of elastodynamic ray theory, is less susceptible to damping effects since these affect wave speeds to a lesser extent than amplitudes. To be useful the pulses must be quite short, or the flaws should be relatively large. The pulses that are generated by mechanisms other than specular reflection may be very small, sometimes so small that they cannot be distinguished from noise that is produced in the system, unless sophisticated data processing techniques are applied.

In general terms, two approaches to ultrasonic flaw detection and characterization have been taken. The imaging approach seeks to process the scattered field in such a manner that a visual outline of the object is produced on a display. The inverse-scattering approach attempts to infer geometrical characteristics of a flaw from either the angular dependence of its far-field scattering amplitude at fixed frequency, or from the frequency dependence of its far-field scattering amplitude at fixed angles.

Imaging is conceptually simple, but difficult to implement with ultrasonic signals. The basic idea is to collect signals scattered by the flaw into an experimentally accessible aperture and then to recombine these signals such that the ones scattered from a particular point on the flaw add coherently at a unique point on the image. At other points in the image, these same signals should not add in phase. Not surprisingly, the main difficulty with imaging is to obtain an acceptable level of resolution. A number of innovative instruments and signal processing methods have been developed. An important example is the acoustic microscope. This instrument was initially developed in the gigahertz frequency regime, where

the wavelength is on the order of a micrometer and resolution approaches that of optical microscopes. The acoustic microscope can, however, also "see" under the surface of a solid, and it can image both microstructure and flaws. Imaging is an important method of detection and characterization, but it falls somewhat outside the scope of this paper. For an interesting discussion of its potential, but also of the current problems with imaging, we refer to the review paper by Thompson and Thompson [2].

In experimental work on quantitative flaw definition by the scattered-field method, either the pulse-echo method with one transducer or the pitch-catch method with two transducers is used. The transducer(s) may be either in direct contact with the specimen, or transducer(s) and specimen may be immersed in a water bath. Most experimental setups include instrumentation to gate out and spectrum analyze the signal diffracted by a flaw. The raw scattering data generally need to be corrected for transducer transfer functions and other characteristics of the system, which have been obtained on the basis of appropriate calibrations. After processing, amplitudes and phase functions, are available as functions of the frequency and the scattering angle. These experimental data can then be directly compared with theoretical results. For the inverse scattering method, the experimental data can be interpreted with the aid of analytical methods, to characterize the scatterer.

In recent years several methods have been developed to investigate scattering of elastic waves by interior cracks as well as by surface-breaking cracks, in both the high- and the low-frequency domains. The appeal of the high-frequency approach is that the probing wavelength is of the same order of magnitude as the length-dimensions of the crack. This gives rise to interference phenomena which can easily be detected. The advantage of the low frequency approach is that useful approximations can be based on static results. A large body of numerical results has been developed for the direct problem of elastodynamic scattering by an inhomogeneity. In particular, several numerical programs based on the use of the T-matrix method and the boundary element method have been developed.

The solution to the direct scattering problem, that is, the computation of the field generated when an ultrasonic wave is scattered by a known flaw, is a necessary preliminary to the solution of the inverse problem, which is the problem of inferring the geometrical characteristics of an unknown flaw from either the angular dependence of the amplitude of the scattered far-field at fixed frequency, or from the frequency dependence of the far-field amplitude at fixed angle. In recent years solutions to the inverse problem have been obtained by the use of nonlinear optimization methods.

Other applications of ultrasonic wave methods, e.g., to acoustic emission techniques and distributed property measurements are not discussed here, due to length limitations. More complete discussions of ultrasonic QNDE methods can be found in recent review papers by Thompson and Thompson [2], Fu [3], and Thompson [4]. The role of elastodynamic scattering problems in quantitative non-destructive evaluation has also been reviewed by, e.g., Gubernatis [5] and Bond et al. [6]. Interesting practical applications have been discussed by Coffey and Chapman [7].

Section 2 starts the main body of this paper with a discussion of the relation between quantitative ultrasonics and strength considerations. The principles and objectives of mathematical modelling both for ultrasonic wave scattering and for static analysis of the fields of stress and deformation near the edge of a crack are discussed in Section 3. Sections 4 and 5 are concerned with two methods for the direct scattering problem: the time domain finite difference method, and ray theory methods.

Corresponding methods for the inverse problem of crack characterization are also briefly discussed. Frequency domain techniques are discussed in Section 6. Most of the results of this Section are based on a representation integral for the scattered displacement field. In Section 7 we discuss an inverse method to characterize a crack of general shape in an elastic solid, by the use of ultrasonic crack-scattering data in conjunction with the integral representation for the scattered-field. For a given set of scattered field data the inverse problem is formulated as a nonlinear optimization problem. For the case of normal incidence discussed in this paper, the solution gives the location of the crack, and the crack-opening volume induced by the probing ultrasonic field. For a problem of quasi-static loading, the Mode-I stress intensity factor induced by the presence of the crack has been computed directly from the results of a related inverse scattering problem. Section 8 is concerned with the effect of near-tip zones of different mechanical properties on the scattered field. Some results for scattering by a partially closed crack are given in Section 9. Effects of the presence of discrete scatterers such as microcracks, voids and inclusions near a crack tip are discussed in Section 10.

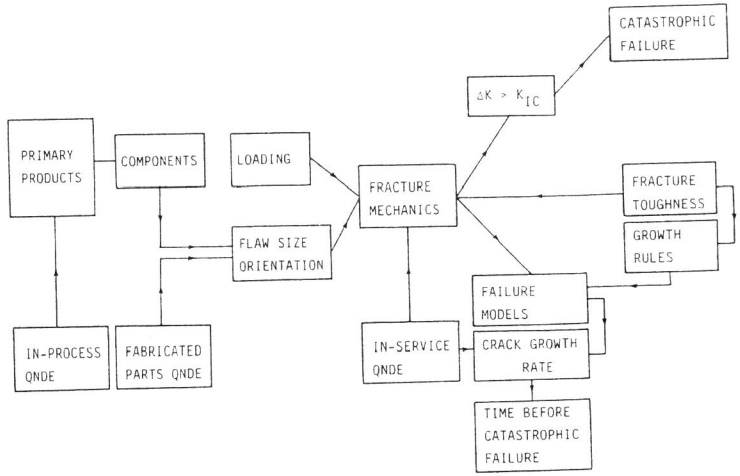

Fig. 2 Role of quantitative non-destructive evaluation in the life-cycle of a component.

2. Strength Considerations

The role of quantitative non-destructive evaluation during the various stages of the life cycle of a structural component is illustrated in Fig. 2. The schematic depiction is meant to apply to metal components which are subjected to cyclic loading, and hence may sustain metal fatigue. As indicated in Fig. 1, Quantitative NDE methods should enter in the material processing stage, to play a role in maintaining material quality of primary products. At this stage QNDE methods ensure that primary products do not contain cracks or other flaws whose dimensions exceed a certain specified level. Plates, sheets and strips are examples of primary metal products that should be inspected and subjected to quality control before being used for the fabrication of parts. In the next stage, QNDE methods should be applied to characterize flaws that have been induced in the process of

fabricating components. The maximum dimensions of such cracks, in conjunction with the magnitude of the cyclic load, can be used to calculate the maximum values of corresponding stress intensity factors. Naturally these maximum values, ΔK, should be less than the fracture toughness. If this is indeed the case, then a crack may still propagate, but at a controlled rate which in principle is predictable. Hence within the framework of the "fail safe" or 'damage tolerant" philosophy, a part containing a macroscopic flaw is acceptable if it can be shown that at the predicted stress levels, the flaw will not grow to critical size during the design lifetime. Reliable quantitative methods of non-destructive in-service inspection of parts are clearly essential for a successful implementation of the damage tolerant philosophy. Flaws which at the time of in-service inspection are greater in size than consistent with the design lifetime, must be detected and characterized. On the other hand the QNDE procedure should not reject components that contain only smaller size flaws. A part should be returned to service if no flaws are found, or if it can be shown that the size of a detected flaw is small enough that it will propagate to failure only over a period substantially larger than the next inspection interval. Very considerable life cycle cost savings can be achieved with this "retirement for cause" procedure. Retirement for cause procedures have been discussed in considerable detail in the literature, see e.g. Refs.[8]-[9].

Clearly, it is extremely important that QNDE procedures, (for the present discussion: ultrasonic techniques) can reliably determine the location, size, shape and orientation of cracks. In the sequel we will discuss the methods and their mathematical background. A more direct connection skips the geometrical crack-characterization stage and attempts to directly determine stress intensity factors under service loads from ultrasonic scattering data. In the remainder of this Section we will discuss this interesting connection between fracture mechanics and scattering of ultrasonic waves, which was noted by Budiansky and Rice [10].

The incidence of ultrasonic waves on a crack generates stress intensity factors along the edge of the crack. The calculation of dynamically induced stress intensity factors is a problem of long-standing interest in dynamic fracture mechanics, see, e.g., [11].

For the sake of simplicity of exposition, let us consider a flat crack of arbitrary shape in the x_1,x_2-plane, and let a plane longitudinal wave of the special form

$$u_3(x_3,t) = \delta(t - x_3/c_L) \tag{1}$$

be incident on the crack. Here $\delta(\cdot)$ is the Dirac delta function and c_L is the longitudinal wave speed. Let the corresponding crack-opening volume be denoted by $V^\delta(t)$. Now, if the incident wave is of the more general form

$$u_3(x_3,t) = f(t - x_3/c_L)\, H(t - x_3/c_L) \quad , \tag{2}$$

it follows immediately by linear superposition that the corresponding crack-opening volume may be written as

$$V(t) = \int_0^t f(t-s)V^\delta(s)ds \tag{3}$$

The asymptotic form of V(t) as time increases, depends on the stress field corresponding to Eq.(2). If the stress component $\sigma_{33}(x_3,t)$ which corresponds to Eq.(2) approaches a finite limit as $t \to \infty$, i.e., as

$$\lim_{t\to\infty} [-(\lambda+2\mu)/c_L]f'(t-x_3/c_L) = \sigma_{33}^{st} \quad , \tag{4}$$

then V(t) also approaches a finite limit, which just equals the static crack-opening volume induced by the static stress σ_{33}^{st}.

Equation (3) is a convolution integral. It is well known that the Fourier transform (over time) of (3), which is indicated by a bar, is of the form

$$\bar{V}(\omega) = \bar{f}(\omega)\bar{V}^\delta(\omega) \quad . \tag{5}$$

It is also known that the long-time value of a quantity is related to the value at small ω of its Fourier transform. It can be shown that

$$\begin{aligned} V^{st} &= \lim_{\omega\to 0} i\omega\, \bar{V}(\omega) \\ &= \lim_{\omega\to 0} i\omega\, \bar{f}(\omega)\bar{V}^\delta(\omega) \\ &= -\frac{c_L}{\lambda+2\mu}\, \sigma_{33}^{st} \lim_{\omega\to 0} \frac{\bar{V}^\delta(\omega)}{i\omega} \end{aligned} \tag{6}$$

Now, if it would be possible to obtain $\bar{V}^\delta(\omega)$ from an ultrasonic test, then V^{st} corresponding to the static stress σ_{33}^{st} could be obtained directly from Eq.(6).

Data obtained from ultrasonic tests generally yield displacements (or their Fourier transforms) at a limited number of points of observation. As shown in the sequel it is possible to extract crack-opening volumes as functions of the frequency from measured displacements, on the basis of elastodynamic modeling formulas. Once a crack-opening volume has been obtained, it is possible to estimate the maximum value of a related static stress intensity factor.

The approach is based on a formula stated by Budiansky and O'Connell [12] which relates the static crack opening volume to the static stress intensity factor by

$$V^{st} = \frac{1-\nu}{3\mu}\, \sigma_{33}^{st} \int_S \rho_c\, [k_I(\ell,\omega)]^2 d\ell \quad , \tag{7}$$

where S is the edge of the crack and ρ_c is a length parameter of the crack. Also, $k_I = K_I/\sigma_{33}^{st}$ is the reduced mode I stress-intensity factor. According to Budiansky and Rice [10] the right hand side of (7) can be approximated by an expression in terms of the maximum value of k_I. This results in

$$V^{st} \simeq \frac{(1-\nu)\pi^3}{24\mu}\, \sigma_{33}^{st}[(k_I)_{max}]^6 \tag{8}$$

or

$$(K_I)_{max} \simeq \left[\frac{24\mu}{(1-\nu)\pi^3} \frac{V^{st}}{\sigma_{33}^{st}}\right]^{1/6} \sigma_{33}^{st} \tag{9}$$

The Fourier transform of a plane longitudinal wave which is incident on the crack in an ultrasonic test, may be written as

$$u_3 = \bar{A}(\omega)e^{ik_L x_3} \quad , \tag{10}$$

If $\bar{V}^u(\omega)$ is the crack-opening volume corresponding to Eq.(10), it follows that

$$\bar{V}^\delta(\omega) = \bar{V}^u(\omega)/\bar{A}(\omega) \tag{11}$$

By substitution of Eq.(11) into Eq.(6), and subsequent substitution of the result in Eq.(9) it then follows that $(K_I)_{max}$ for a service condition can be obtained from the ultrasonic test data as

$$(K_I)_{max} = \left[\frac{-24c_L}{(1-\nu)\pi^3}\frac{\mu}{\lambda+2\mu}\lim_{\omega\to 0}\frac{\bar{V}^u(\omega)}{i\omega\bar{A}(\omega)}\right]^{1/6}\sigma_{33}^{st} \tag{12}$$

In another connection with fracture analysis, ultrasonic methodology for determining the fracture toughness of structural materials is of high interest, see [13]-[14]. A major incentive is the need for rapid, inexpensive, and nondestructive methods for verifying fracture toughness and related mechanical properties prior to placing critical parts in service and after the parts have been exposed to service.

Fracture toughness is an extrinsic mechanical property. It is a measure of a material's fracture resistance that quantifies the stress intensity at which a particular size crack becomes unstable and grows catastrophically. It is known that fracture toughness is governed by microstructure and morphology in polycrystalline solids. Because the attenuation of ultrasonic waves is also governed by similar factors, one should expect correlations between toughness and ultrasonic properties of polycrystallines.

Prior works have presented empirical evidence of correlations between ultrasonic attenuation measurements and fracture toughness in polycrystalline solids. A theoretical basis has been suggested for the correlations found between ultrasonic attenuation and fracture toughness.

The viability of ultrasonics for verifying fracture toughness of materials and components is being investigated. Thus far, correlations of ultrasonic measurements with toughness have been demonstrated only on laboratory samples of polycrystalline solids. Further work is needed to establish underlying principles and appropriate approaches for applications to a variety of materials and hardware configurations.

In still another connection between ultrasonics and fracture, ultrasonic measurements of asperity contacts on the crack faces have been analyzed to determine crack tip shielding from the externally applied driving force, by Buck et al [15].

3. Mathematical Modelling

Mathematical modelling of ultrasonic wave scattering provides valuable quantitative information for methods to detect and characterize cracks. Even though both the geometrical configuration and the process of ultrasonic wave propagation must be simplified to accommodate a mathematical approach, the characteristic features of the scattering phenomenon can be maintained. Results obtained by the modelling approach aid in the design of efficient testing configurations, as well as in the interpretation of experimental results and field data. Mathematical

modelling in NDT, what it is and what it does, has been discussed in some detail by Coffey [16].

Once a mathematical model has been verified by comparisons with a sufficiently wide range of experimental data, it can play an extremely important role, in that representative synthetic data can be generated with very little effort. This is particularly important in the generation of a knowledge base for an expert system.

In recent years numerous results have become available for fields generated by scattering of ultrasonic waves by flaws. Solutions are available for scattering by voids, inclusions, internal cracks, macrocrack-microcrack configurations, arrays of cracks and surface breaking cracks. Most results are in the frequency domain, but they can be converted to the time domain by application of the Fast Fourier Transform. Recently numerical results have been developed directly in the time domain.

In a homogeneous, isotropic, linearly elastic solid, the components of the displacement vector are governed by

$$(\lambda+\mu)\underset{\sim}{\nabla}\,\underset{\sim}{\nabla}\cdot\underset{\sim}{u} + \mu\nabla^2\underset{\sim}{u} = \rho\ddot{u} \tag{13}$$

where λ and μ are elastic constants, and ρ is the mass density. This equation must be supplemented by appropriate initial and boundary conditions. The boundary conditions must be satisfied on the external boundaries of the body and on the faces of the crack.

Analytical and numerical results are generally obtained for a perfect mathematical crack. The faces of a perfect mathematical crack are smooth and infinitesimally close, but they are specified not to interact with each other. From the analytical point of view a perfect mathematical crack is a surface in space which does not transmit tractions. The model is acceptable for a real crack, provided that the latter's faces are slightly separated and that the length characterizing crack-face roughness is much smaller than the dominant wavelengths of an incident pulse of ultrasonic wave motion.

There are few exact closed-form analytical solutions to elastodynamic scattering problems. In a rigorous approach, often the best that can be done is to reduce the mathematical formulation to a form which is suitable for numerical work. Closed-form solutions can be obtained at high frequencies (Kirchhoff approximation or geometrical diffraction theory) [17] or at low frequencies (Rayleigh approximation) [18]. However these approximations are of limited value for scattering in the mid-frequency range in which characteristic wavelengths of an incident displacement pulse are of the same order of magnitude as a characteristic length of the flaw. In that range it is necessary to use numerical methods; for example, numerical schemes to solve systems of governing integral equations, finite difference techniques, finite element techniques, T-matrix methods, etc. Typical of the latter is the work of Visscher [19] and Opsal and Visscher [20].

As shown in Ref.[21], the effect of a crack on an incident field of ultrasonic wave motion can be nicely displayed in full-field snapshots, with the aid of time-domain finite difference calculations. Some results are shown in Section 4. Other results obtained by the finite difference method can be found in Refs.[22]-[25]. For crack characterization, only the fields at a few well selected points of observation are, however, generally required. These are generally more efficiently calculated by the use of the boundary element method, which can also be used when the crack is not perfect.

In the frequency domain, the exact formulation of elastodynamic scattering problems results in the statement of a set of singular integral equations. For scattering by cracks, the unknown quantity in the integral equations is the crack-opening displacement. Generally, the integral equations must be solved numerically. Two methods can be used to obtain the set of singular integral equations: Fourier transform techniques and Green's functions methods provide an effective approach.

In recent years numerous results have become available for fields generated by scattering of ultrasonic waves by cracks. Solutions for two-dimensional configurations in unbounded bodies have been discussed by Achenbach, et al [17], who also listed earlier references. The three-dimensional case of scattering of a plane wave by a penny-shaped crack has been investigated in Refs.[26]-[30]. Scattering by a crack of elliptical shape was investigated in Ref.[31]. The more difficult configurations of a surface-breaking and a sub-surface crack have been considered in Refs.[32]-[38]. Three-dimensional scattering by a surface-breaking crack has been analyzed by Angel and Achenbach [39] and Budreck and Achenbach [40]. For the surface breaking crack comparisons between the analytical results and experimental data have been presented by Yew et al. [41], Dong and Adler [42] and Vu and Kinra [43]. Experimental results for reflection of a surface wave by a sub-surface crack oriented normal to the free surface were obtained by Khuri-Yakub et al. [44], who observed very satisfactory agreement with the theoretical results. Recently, results directly in the time domain have also been obtained by the boundary element method, see Refs.[45]-[46].

In recent work Achenbach et al [47], analytical modeling has been improved by including a number of aspects typical of practical configurations. Thus, it was taken into account that the transmitting and receiving transducers are often coupled to the specimen by placement in a water bath. The transmission of the signal from the water to the solid requires careful investigation. It was also taken into account that only part of the crack may be illuminated by the incident signal. The relation between the scattered field and the electrical signal recorded by the receiving transducer was made part of the overall approach by directly relating this signal to the crack-opening displacement which is generated by the incident wave. The crack-opening displacement was computed by the use of the frequency-domain methods developed earlier. The process of modeling from the initial electrical pulse to the measured electrical pulse included conversion to the time-domain by the use of the fast Fourier transform method. Reference [47] shows results in the time and frequency domains.

Real cracks, particularly fatigue and stress corrosion cracks have rough faces, which may contact each other. Sometimes there is not a single crack, but rather a configuration of a principal crack and an adjoining sattelite crack, e.g., a macrocrack and a neighboring microcrack. It also frequently happens that other smaller scatterers such as voids and inclusions are located near a crack. The secondary scattering from these inhomogeneities will affect the overall scattered field. Still another complicating factor may be introduced by the presence of small zones of different material properties at the crack tips. In this paper we report some analytical results which account for these complicating features of real cracks, with a view towards predicting their effects in actual testing situations.

The calculation of the fields of stress and deformation in a cracked body under static loading conditions, is mathematically almost completely analogous to scattered field calculations for ultrasonic wave incidence. From the point of view of fracture, the near-field is of interest while for ultrasonic scattering the far-field is most relevant. In fracture mechanics the emphasis is on stress-intensity factors which define the

fields near the edge of a crack. It is, however, not surprising that the stress intensity factors generated by static service loads can be related to the scattered field generated by the incidence of ultrasonic pulses. This relation, and its relevance to strength assessment of a body containing a crack is discussed in Ref.[48] and Sections 2 and 7.

4. Time-Domain Finite Difference Calculations

Reference [21] presents solutions to Eq.(1) that have been obtained by the finite difference method. The finite difference method used is explicit in time. In Ref.[21], use is made of previously unreported difference formulations for some of the special nodes contained in the numerical domain. A radiation condition which allows free transmission of energy from the numerical domain for body waves as well as surface waves was successfully employed.

The configuration is shown in Fig. 1 of Ref.[21]. A transducer on the upper face of the slab generates a transverse wave which propagates towards the surface-breaking crack. All fields are taken as independent of z, which reduces the problems to ones of two-dimensional plane-strain scattering.

The transducer has been simulated by choosing the surface tractions in such a way that they produce a beam of transverse wave motion, of finite width and finite duration, which traverses the slab at a 45^0 angle, and is directed towards the mouth of the surface-breaking crack. The transverse displacement pulse illustrated in Fig. 1(b) was used. The tractions applied at the transducer/slab interface correspond to those for a pulse in an unbounded medium of the form shown in Fig. 1(b), which passes the interface "window" and produces tractions along the interface. These are just the values used in the numerical simulation. Since the plane wave passes the interface at a 45^0 angle no shear tractions are induced. A time delay is incorporated into the incident pulse so that at the onset of the numerical iterations, displacements and particle velocities may be set to zero.

To complete the formulation of the problem, conditions at the ends of the slabs must be specified. As the slabs are semi-infinite in extent, the displacement waves are outgoing. Hence, in the truncated numercial domain a radiation condition is employed.

The numerical results are displayed in two ways, (1) spatial displacement distributions (snapshots) at a specified time, and (2) time histories of the normal component of the particle velocity at the midpoint of the transducer/plate interface. A spatial displacement distribution is obtained by depicting displacements by vectors emanating from the corresponding nodal points, but only at nodes where the displacement magnitude is greater than a specified value. This yields a snapshot of the displacement distribution generated by scattering of the incident pulse, both in magnitude and direction. The normal component of the particle velocity at the midpoint of the transducer/plate interface has been chosen for the time-history display.

Figure 5 of Ref.[21] compares the time histories of the normal velocity at the midpoint of the transducer/plate interface, for the cases with and without a crack. The most obvious differences are the sharp peaks centered around 30 μs for the plate with a crack. This pulse represents the reflection of the transverse pulse by the crack faces. The velocity of the incident pulse caused by the tractions applied at the transducer interface is represented by the peaks centered around 7.5 μs. A small peak near 25 μs can be identified as the diffraction from the crack tip. The difference

in arrival times of the two signals can be used to compute the depth of the crack by a simple formula, see e.g., Refs.[49]-[52].

5. Ray Methods

In ray theory it is assumed that disturbances propagate along straight or curved rays, and that the interaction of rays with inhomogeneities follows simple geometrical rules which can be established on the basis of solutions to canonical problems. If the rules are known, then rays can be traced and (in principle) the signals that propagate along all rays passing through a point of observation can be superimposed to yield the complete field. The geometrical aspects of ray theory have intuitive appeal, and they are relatively simple. From the mathematical point of view, ray theory gives an expansion which has asymptotic validity with respect to "high" frequency or "small" time after arrival of a disturbance.

The scattering of a bundle of rays by a crack-like flaw follows relatively simple rules. At sufficiently high frequencies, diffraction at certain points on the crack edge, which have been called the "flash points", produces the dominant part of the scattered field. The flash points emit bundles of diffracted waves which propagate towards a point of observation. The basic theory has been presented in Ref.[17].

The theory of elastodynamic crack-edge diffraction is based on the result that two cones of diffracted rays are generated when a ray carrying a high-frequency elastic wave strikes the edge of a crack. The inner and outer cones consist of rays of longitudinal and transverse motion, respectively. For cracks in elastic solids, the three-dimensional theory of edge diffraction was discussed by Achenbach et al [17].

Comparison of theoretical ray theory results with experimental results has been given in Ref.[53].

In the direct problem the incident wave and the geometrical configuration are known. For a given point of observation the positions of the flash points on the crack edge can then be determined by geometrical considerations, and the scattered field can subsequently be determined by direct ray tracing. If the geometrical configuration is unknown, but information is available on the diffracted field, an inverse ray tracing procedure can be used to determine the flash points on the crack edge from which diffracted signals have emanated.

In recent papers, see e.g.[54], two analytical methods have been developed to map the edge of a crack by the use of data for diffraction of elastic waves by the crack-edge. These methods of Ref. [54] are based on elastodynamic ray theory and the geometrical theory of diffraction, and they require as input data the arrival times of diffracted ultrasonic signals. The first method maps flash points on the crack edge by a process of triangulation with the source and receiver as given vertices of the triangle. By the use of arrival times at neighboring positions of the source and/or the receiver, the directions of signal propagation, which determine the triangle, can be computed. This inverse mapping is global in the sense that no a-priori knowledge of the location of the crack edge is necessary. The second method is a local edge mapping which determines planes relative to a known point close to the crack edge. Each plane contains a flash point. The envelope of the planes maps an approximation to the crack edge.

In Ref. [54] the material containing the crack was taken as a homogeneous, isotropic and linearly elastic solid. More recently, extensions to include anisotropy of the material have been given in Ref. [55].

Mathematical details and a fairly detailed error analysis can be found in Ref.[54]. The reference also includes applications of the methods to synthetic data. It is of particular interest that the local mapping technique allows for an iteration procedure whereby the result of a computation suggests an improved choice of the base point which in the subsequent iteration yields a better approximation to the crack edge. A comparison with experimental data has been given in Ref.[56].

6. Frequency-Domain Analysis

It is a well-known result of classical elastodynamic analysis that the scattered field generated by incidence of an ultrasonic wave on an inhomogeneity in an elastic solid, can be expressed by a representation integral. The integral, which is defined either over the surface of the inhomogeneity or over its interior domain, relates the field at a specified point in the body to the fields on or inside the inhomogeneity, via Green's function terms in the integrands. In a rigorous approach to the solution of the scattering problem, the boundary conditions in conjunction with a limiting process on the surface integral as the field point approaches the surface of the scatterer, give rise to a set of integral equations for the unknown fields on the surface of the inhomogeneity. The set of integral equations must generally be solved by a numerical method, such as the boundary element method, see, e.g. Kitahara et al.[57]. In a related approximate approach the fields on or in the scatterer are not calculated rigorously, but for certain special cases (low frequency, weak scatterer, high frequency) they are approximated for direct use in the representation integral.

For scattering of time harmonic waves by an inhomogeneity, the field exterior to the inhomogeneity may be written as the sum of the incident and scattered fields,

$$\underset{\sim}{u}(\underset{\sim}{x}) = \underset{\sim}{u}^{I}(\underset{\sim}{x}) + \underset{\sim}{u}^{S}(\underset{\sim}{x}) \quad . \tag{14}$$

Note that here and in the sequel the time-harmonic term $\exp(-i\omega t)$ is being omitted. In this Section we will consider two special cases for the scattering inhomogeneity: an inclusion and a crack.

First scattering by an inclusion. To distinguish the fields outside the inclusion (in the matrix material) from those inside the inclusion we use the following notation

$$\text{matrix:} \qquad \underset{\sim}{u}(\underset{\sim}{x}),\ c_L, c_T,\ C_{ijpq}, \rho \tag{15}$$

$$\text{inclusion:} \qquad \bar{\underset{\sim}{u}}(\underset{\sim}{x}),\ \bar{c}_L, \bar{c}_T,\ \bar{C}_{ijpq}, \bar{\rho} \tag{16}$$

Here $\underset{\sim}{u}(\underset{\sim}{x})$ defines the <u>total</u> displacement field, ρ is the mass density, and c_L and c_T are the velocities of longitudinal and transverse waves, respectively. The constants C_{ijpq} are the elastic constants which appear in the generalized form of Hooke's law. For an isotropic material we have

$$C_{ijpq} = \lambda\delta_{ij}\delta_{pq} + \mu(\delta_{ip}\delta_{jq} + \delta_{iq}\delta_{jp}) \quad , \tag{17}$$

where λ and μ are Lame's elastic constants and δ_{ij} is the Kronecker delta.

It has been shown elsewhere, see e.g.[58], that the scattered field at a position defined by a position vector $\underset{\sim}{x}$ in the matrix material may be expressed as

$$u_k^S(\underset{\sim}{x}) = \int_V \delta C_{ijpq} \frac{\partial U_{ik}(\underset{\sim}{x}-\underset{\sim}{\xi})}{\partial x_j} \frac{\partial \bar{u}_p(\underset{\sim}{\xi})}{\partial \xi_q} dV(\underset{\sim}{\xi}) + \omega^2 \int_V \delta\rho\, U_{ik}(\underset{\sim}{x}-\underset{\sim}{\xi})\bar{u}_i(\underset{\sim}{\xi})dV(\underset{\sim}{\xi}), \quad (18)$$

where

$$\delta C_{ijpq} = \bar{C}_{ijpq} - C_{ijpq}, \quad \delta\rho = \bar{\rho}-\rho, \quad (19a,b)$$

and $U_{ik}(\underset{\sim}{x}-\underset{\sim}{\xi})$ is the fundamental solution of elastodynamics for the matrix material. This solution represents the displacement in the x_i-direction, due to a unit load in the x_k-direction applied at position $\underset{\sim}{x} = \underset{\sim}{\xi}$. Also, V is the volume of the inclusion, and repeated indices imply summation.

Next we consider scattering by a crack. It is well-known, [17], that the scattered field may be expressed as

$$u_k^{Sc}(\underset{\sim}{x}) = -\int_S C_{ijpq} \frac{\partial U_{pk}(\underset{\sim}{x}-\underset{\sim}{\xi})}{\partial \xi_q} \Delta u_i(\underset{\sim}{\xi}) n_j(\underset{\sim}{\xi}) dA(\underset{\sim}{\xi}) \quad . \quad (20)$$

Here S denotes the insonified face of the crack, $\underset{\sim}{n}(\underset{\sim}{\xi})$ is the normal to the crack plane and $\Delta u_i(\underset{\sim}{\xi})$ is the crack-opening displacement,

$$\Delta u_i(\underset{\sim}{\xi}) = u_i^{Sc}(\underset{\sim}{\xi}^+) - u_i^{Sc}(\underset{\sim}{\xi}^-) \quad . \quad (21)$$

where $\underset{\sim}{\xi}^+$ and $\underset{\sim}{\xi}^-$ are position vectors of corresponding points on the insonified and shadow faces of the crack. It should be noted that Δu_i may equally well be expressed as the discontinuity in the <u>total</u> displacement, since the incident field is continuous across the crack faces.

A set of boundary integral equations can be derived by substituting Eq.(20) into Hooke's law and by considering the stress free boundary conditions on the crack faces. In general, these boundary integral equations must be solved numerically, for example by the boundary element method. Details can be found in a recent paper by Zhang and Achenbach [59]. Applications to various kinds of cracks can be found in Refs.[29]-[31], [37]-[38] and [40].

7. Crack Characterization by Ultrasonic Scattering Methods

In a recent paper, [48], an inverse method has been proposed which employs ultrasonic crack-scattering data to characterize a crack of general shape and orientation in a homogeneous, isotropic, linearly elastic solid. The method is based on the integral representation for the scattered field given by Eq.(20).

For a crack in the x_1x_2-plane, and for normal incidence, i.e., the incident wave propagates in the x_3-direction, Eq.(20) may be rewritten as

$$u_k^{Sc}(\underset{\sim}{x}) = \int_A C_{33\ell m} D_{k\ell m}(\underset{\sim}{x}-\underset{\sim}{\xi})\Delta u_3(\underset{\sim}{\xi})dA(\underset{\sim}{\xi}) \quad (22)$$

where

$$D_{k\ell m}(\underset{\sim}{x}-\underset{\sim}{\xi}) = \frac{\partial}{\partial x_m} U_{k\ell}(\underset{\sim}{x}-\underset{\sim}{\xi}) \quad (23)$$

As noted in the previous section, $U_{k\ell}(\underset{\sim}{x}-\underset{\sim}{\xi})$ is the displacement at position $\underset{\sim}{x}$ in the direction x_k due to a unit force applied in the direction x_ℓ at $\underset{\sim}{x}=\underset{\sim}{\xi}$. Equation (23) then implies that $-D_{k\ell m}(\underset{\sim}{x}-\underset{\sim}{\xi})$ is the displacement produced at position $\underset{\sim}{x}$ in the x_k-direction, by a double force applied at $\underset{\sim}{x}=\underset{\sim}{\xi}$ with forces in the x_ℓ-direction and moment arm in the x_m-direction.

In the far-field ($k_\alpha|\underset{\sim}{x}-\underset{\sim}{\xi}| \gg 1$, α = L,T) and for relatively low frequencies ($k_\alpha a \ll 1$, where a is a characteristic length dimension of the crack), Eq.(22) may be simplified to

$$u_k^{Sc}(\underset{\sim}{x}) = C_{33\ell m} D_{k\ell m}(\underset{\sim}{x}) V_{33} \quad (24)$$

where

$$V_{33} = \int_A \Delta u_3(\underset{\sim}{\xi})dA(\underset{\sim}{\xi}) \quad (25)$$

is the crack-opening volume, and the origin of the coordinate system is taken at the centroid of the crack. For an isotropic solid $C_{33\ell m}$ follows from Eq.(17), and Eq.(22) may be written as

$$u_k^{Sc}(\underset{\sim}{x}) = L_{k33}(\underset{\sim}{x}) V_{33} \quad (26)$$

where $L_{k33}(\underset{\sim}{x})$ is defined in Ref.[48].

Physically, the scattered field of Eq.(24) can be thought of as being produced by three double forces (force and arm in the same direction) in the x_1,x_2 and x_3 directions, located at the centroid of the crack, and of strength λV_{33}, λV_{33} and $(\lambda+2\mu)V_{33}$, respectively.

Now suppose that the three displacement components of the scattered field have been measured at a point of observation $\underset{\sim}{x}$. If the origin of the coordinate system is placed on the crack, then the coordinates of the point of observation become unknown, since the location of the crack is unknown. The displacements are complex valued, and hence Eq.(26) defines a set of six nonlinear equations for five unknowns, namely, for the 3 components of $\underset{\sim}{x}$ and the real and imaginary parts of V_{33}. It follows that Eq.(26) is an overdetermined set of nonlinear equations. The system can, however, be solved numerically, as will be discussed next.

First we eliminate V_{33}, which appears linearly, from the equation for $u_1^{Sc}(\underset{\sim}{x})$. Substitution of the result in the remaining four equations gives

$$\begin{Bmatrix} u_2^{Sc}(\underset{\sim}{x}) \\ u_3^{Sc}(\underset{\sim}{x}) \end{Bmatrix} - \frac{u_1^{Sc}(\underset{\sim}{x})}{L_{133}(\underset{\sim}{x})} \begin{Bmatrix} L_{233}(\underset{\sim}{x}) \\ L_{333}(\underset{\sim}{x}) \end{Bmatrix} \quad (27)$$

Equations (27) define a system of four equations and three unknowns (the components of $\underset{\sim}{x}$). The solution is obtained by solving a nonlinear optimization problem with residuals of the form

$$g_1(\underset{\sim}{x}) = \mathrm{Re}[u_2^{Sc}(\underset{\sim}{x})] - \mathrm{Re}\left[\frac{L_{233}(\underset{\sim}{x})}{L_{133}(\underset{\sim}{x})} u_1^{Sc}(\underset{\sim}{x})\right] \quad (28)$$

$$g_2(\underset{\sim}{x}) = \mathrm{Re}[u_3^{Sc}(\underset{\sim}{x})] - \mathrm{Re}\left[\frac{L_{333}(\underset{\sim}{x})}{L_{133}(\underset{\sim}{x})} u_1^{Sc}(\underset{\sim}{x})\right] \quad (29)$$

and two more residuals for the corresponding imaginary parts. The four residuals $g_i(\underset{\sim}{x})$ are minimized in the least squares sense with respect to $\underset{\sim}{x}$, i.e., we seek

$$\underset{\underset{\sim}{x}}{\mathrm{Min}} \sum_{i=1}^{4} g_i^2(\underset{\sim}{x}) \quad (30)$$

The nonlinear least squares problem can be solved numerically by the Levenberg-Marquardt algorithm, as discussed in some detail in Ref.[48].

Once the three components of $\underset{\sim}{x}$ have been obtained, V_{33} can be calculated from Eq.(26).

As discussed earlier in this paper, the ultimate aim of quantitative non-destructive evaluation is to obtain information on the residual strength of components. By combining the information on the crack opening volume, obtained in the manner described in this section, with the approach of Section 2, it is possible to estimate the maximum stress intensity factor. This will require a low frequency limit of the crack-opening volume, as stated by Eq.(6). Such a low frequency limit may be difficult to obtain directly from experimental data. The general dependence on frequency as the limit of zero frequency is approached is, however, known from analytical results [18], and this should help to determine the required limit.

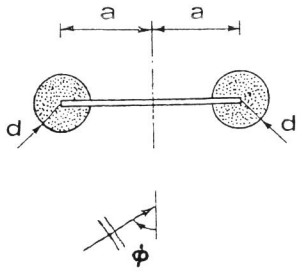

Fig. 3 Scattering by a crack with near-tip zones of different mechanical properties.

8. Effect of Near Tip Zones

Scattering by a crack with regions of different mechanical properties surrounding its crack tips has been investigated in some detail in Ref.[61]. The two-dimensional configuration is shown in Fig. 3. To apply Eqs.(18) and (20) to two-dimensional problems, the volume integration in Eq.(18) becomes an integration over an area A, while the surface integration over S in Eq.(20) becomes an integration over a crack line Γ. In addition the indices range over 1 and 2 only, the deformation is in plane strain and the fundamental solution is two-dimensional.

It is now not difficult to show that the scattered field may be expressed as the superposition of Eq.(20) and two integral expressions of the general form (22) for the two crack-tip regions. Before we give the expressions we will, however, introduce some simplifications, which are based on the following order of magnitude observations, see Fig. 3,

$$((x_1 \pm a)^2 + x_2^2)^{\frac{1}{2}}/d \gg 1 \qquad (31)$$

and

$$k_L d \ll 1 \quad . \qquad (32)$$

where d is a characteristic length of the crack-tip regions. Under these assumptions, $U_{ik}(\underset{\sim}{x}-\underset{\sim}{\xi})$ in Eq.(18) may be brought outside the integral sign and written as

$$U_{ik}(\underset{\sim}{x};\underset{\sim}{\xi}) \simeq U_{ik}(\underset{\sim}{x};\pm a) \qquad (33)$$

We also consider the case that δC_{ijpq} is uniform, and that any variation in the mass density may be ignored, i.e., $\delta\rho = 0$. The total scattered field may then be expressed as

$$u_k^S(\underset{\sim}{x}) = \delta C_{ijpq} \frac{\partial U_{ik}(\underset{\sim}{x};-a)}{\partial x_j} I_{pq}^{\ell} + \delta C_{ijpq} \frac{\partial U_{ik}(\underset{\sim}{x};+a)}{\partial x_j} I_{pq}^{r} + u_k^{Sc}(\underset{\sim}{x}), \qquad (34)$$

where

$$I_{pq}^{\ell,r} = \int_{A_{\ell,r}} \frac{\partial \bar{u}_p(\underset{\sim}{\xi})}{\partial \xi_q} dA(\underset{\sim}{\xi}) \quad . \qquad (35)$$

Here A_ℓ and A_r are the areas near $x_1 = -a$ and $x_1 = a$ respectively, see Fig. 3.

Equation (34) would explicitly define the scattered field if the crack opening displacement, Δu_i, and the displacement gradients, $\partial \bar{u}_p(\underset{\sim}{\xi})/\partial \xi_q$, would be known a-priori. Unfortunately that is not the case. These quantities must generally be obtained by a numerical solution of a set of integral equations that can be derived from the representation integral, as discussed in Section 6. Such a numerical calculation is, however, very cumbersome, and we follow, therefore, an alternative approximate method. This method is valid when the elastic constants of the crack-tip regions are not too different from those of the matrix material. It is assumed that for such weak scatterers the contribution of Δu_i to the integral in Eq.(20) may be approximated by the crack-opening displacement that would pertain in the absence of crack-tip regions . Crack opening displacements for a solitary crack have been calculated, among others, by Zhang and Achenbach [59].

The approximate procedure is also followed for the calculation of the integrals $I_{pq}^{\ell,r}$, defined by Eq.(35). Each displacement gradient in Eq.(11) then has two parts: one for the incident wave field, and one for the field scattered by the crack in the absence of the crack-tip regions. The approximation of the field in an inhomogeneity by the field that would pertain in its absence is essentially the Rayleigh-Gans or Born approximation. For scattering by an inclusion this approximation has been found acceptable for weak scatterers, see e.g. Gubernatis et al.[60].

As a final simplification we push the approximation one step further by including in the near-tip scattered displacement fields only those terms whose displacement gradients contain square-root singular terms. This simplification is acceptable for $d/a \ll 1$ and $k_L d \ll 1$. The near-tip scattered displacements near the right-hand tip are then given by the well-known formulas

$$\begin{Bmatrix} -S \\ u_1 \\ -S \\ u_2 \end{Bmatrix} = \frac{K_I^r}{2\mu}\left(\frac{r}{2\pi}\right)^{1/2}\begin{Bmatrix}(\kappa-\cos\beta)\cos\frac{1}{2}\beta \\ (\kappa-\cos\beta)\sin\frac{1}{2}\beta\end{Bmatrix} + \frac{K_{II}^r}{2\mu}\left(\frac{r}{2\pi}\right)^{1/2}\begin{Bmatrix}(2+\kappa+\cos\beta)\sin\frac{1}{2}\beta \\ (2-\kappa-\cos\beta)\cos\frac{1}{2}\beta\end{Bmatrix}, \quad (36)$$

where K_I^r and K_{II}^r are the Mode-I and Mode-II stress intensity factors at $x_1 = +a$, r is the radial distance from the crack-tip, and β is the polar angle. For plane strain $\kappa = 3 - 4\nu$, where ν is Poisson's ratio. The stress-intensity factors K_I^r and K_{II}^r for the crack under the influence of an incident wave must also be numerically calculated by the same method as Δu_i, see Ref.[59].

Substitution of Eq.(36) into Eq.(35) and subsequent integration yields

$$I_{pq}^{rS} = \frac{1}{3\mu}\left(\frac{2d^3}{\pi}\right)^{1/2}\begin{cases} -K_I^r(\kappa-7/5) & , p=q=1 \\ K_{II}^r(\kappa+13/5) & , p=1, q=2 \\ -K_{II}^r(\kappa-3/5) & , p=2, q=1 \\ K_I^r(\kappa-3/5) & , p=2, q=1 \end{cases}, \quad (37)$$

where the superscript "S" indicates the scattered-field contribution. The results for the left crack-tip region have similar forms

For an incident plane longitudinal wave of the form

$$u_i^I = U_L\begin{Bmatrix}\sin\phi \\ \cos\phi\end{Bmatrix}\exp[ik_L(x_1\sin\phi + x_2\cos\phi)] \quad , \quad (38)$$

where U_L is the amplitude and ϕ is the angle of incidence with the x_2-axis, the contribution of the incident field to (35) is

$$I_{pq}^{rI} = ik_L U_L \pi d^2 \exp(ik_L a\sin\phi)\begin{cases}\sin^2\phi & , p=q=1 \\ \sin(2\phi)/2 & , p\neq q \\ \cos^2\phi & , p=q=2\end{cases} \quad (39)$$

The results of Ref.[61] suggest that for an incident longitudinal wave the effect of near-tip regions is negligible for $\phi < 30^0$, because the scattering by the near tip regions is dominated by crack scattering. Near $\phi \sim 47^0$ the effect is of some significance, and it becomes more important as ϕ increases beyond 60^0, because both scattering effects become of the same order of magnitude. The backscattering from the crack becomes very small for larger values of ϕ, and hence, from the practical point of view it may be very difficult to measure any backscattering at all. For an incident transverse wave the largest effect is observed near $\phi \simeq 35^0$, where the near-tip regions cause an increase in the scattered field of about 11%.

9. Scattering by a Partially Closed Crack

The perfect mathematical crack model is acceptable for a real crack with slightly separated crack faces, and provided that the length characterizing crack-face roughness is much smaller than the dominant wave length of the incident pulse of ultrasonic wave motion. If the crack faces are in contact, and the crack is actually partially closed, the model must be adjusted. In this section we consider the case that the crack is tightly closed over a segment of the crack-surface, so that it can be represented by a configuration of two neighboring cracks.

A mathematical treatment of scattering by a two-dimensional configuration of neighboring cracks has been presented by Zhang and Achenbach [59]. The

results of that paper show that the backscattered displacement is considerably smaller for the partially closed crack. Other results on the effect of crack-face contact on the reflection and scattering of ultrasonic waves can be found in Refs.[61]-[65].

10. The Effects of Near-Tip Satellite Scatterers

Finally, we consider two-dimensional configurations consisting of a principal crack and either a near-tip microcrack, a microvoid or a micro-inclusion. Scattering of ultrasonic waves by such a composite configuration can also be investigated by reducing the problem formulation to a set of singular integral equations, and by subsequently solving these equations by the use of the boundary element method. Results for the backscattered displacement for normal incidence of a longitudinal wave have been presented in Ref.[61], for dimensions of the satellite scatterer which are relatively small as compared to the length of the crack (b/a = 0.05). The difference between the scattered fields appears to be insignificant except when the satellite scatterer would be located very close to the crack tip. Of course, if there is a multitude of satellite scatterers. the backscattered field may become affected in a significant manner.

11. Concluding Comments

Fracture mechanics, or in a more general sense failure mechanics, has made great strides in the prediction of the integrity of structural components. The advances in methods for quantitative strength prediction will, however, not reach their full potential until reliable non-destructive methods are fully utilized to assess the material state and characterize internal flaws, for primary products, fabricated components, and for in service conditions.

This paper has discussed some of the ultrasonic methods that are currently available, or that are in an advanced research state, particularly with regard to strength assessment of bodies that may contain cracks. Particular attention was devoted to direct links between quantitative ultrasonics and strength considerations. Some topics that are just started to be investigated have, however, not been discussed in great detail. Among these we mention expert systems for flaw detection and characterization. Research in this area integrates sensor development, predictive failure analysis and decision making procedures, based on artificial intelligence and expert systems. It is expected that mathematical modelling and analytical results will play an important role in the development of knowledge bases for expert systems.

We conclude this paper with a comment on the concept of integrated life cycle engineering which places quantitative ultrasonics and fracture mechanics, together with design methodology and manufacturing methods in the much broader context of the life cycle of components and structures. The aim of integrated life cycle engineering is to develop an integrated approach towards design and manufacturing based on simultaneous optimization of product performance, manufacturability, reliability, maintainability and life cycle costs during the design development. A reliable method for designed-in structural integrity is an important component of life cycle engineering. The method should include ways for the designer to deal systematically and coherently with stress analysis, critical flaw concepts and flaw detection and characterization, NDE inspectivity, overall design reliability and maintainability, in-service inspection and rational trade-offs between overall reliability and life cycle costs. Quantitative non-destructive evaluation provides the measurement tools and techniques for inspections at various stages of processing, manufacturing and service. Probability of detection models,

smart sensors, automated inspection procedures, methods to characterize imperfections and retirement for cause procedures play essential roles. It is hoped that this paper has illustrated the importance of incorporating QNDE methodology in the integrated life cycle engineering approach.

ACKNOWLEDGMENT

This work was carried out in the course of research for Contract DE FG02-86-ER13484 with the Department of Energy, Office of Basic Energy Sciences, Engineering Research Program and for Contract N00014-85-K-0401 with the Office of Naval Research, Mechanics Program.

REFERENCES

1. P. Höller, In: Nondestructive Characterization of Materials II (eds.J.F. Bussière, J.-P. Monchalin, C.O. Ruud and R.E. Green, Jr.), p. 211, Plenum Press, 1987.
2. R.B. Thompson and D.O. Thompson: Proc. of the IEEE, 1985, vol. 73, p. 1716.
3. L.S. Fu: Applied Mechanics Reviews, 1982, vol. 35, p. 1047.
4. R.B. Thompson: J. Appl. Mech., vol. 50, (50th Anniversary Issue), 1983 p.1191.
5. J.E. Gubernatis, in Review of Progress in Quantitative Nondestructive Evaluation, Vol. 5 (eds. D.O. Thompson and D.E. Chimenti), p. 21, Plenum, New York, 1986.
6. L.J. Bond, M. Punjani and N. Saffari: IEEE Proceedings, 1984, vol. 131, p. 265.
7. J.M. Coffey and R.K. Chapman: Nucl. Energy, 1983, vol. 22, p. 319.
8. J.E. Allison, J.M. Hyzak and W.H. Reimann, in Preventions of Structural Failure (ed. W. Lewis), p. 240, Am. Soc. of Metals, Metals Park, Oh., 1978.
9. C.G. Annis, Jr., M.C. Van Wanderham, J.A. Harris, Jr. and D.L. Sims: J. Eng. for Power, 1981, vol. 103, p. 198.
10. B. Budiansky and J.R. Rice: J. Appl. Mechs. 1978, vol. 45, p. 453.
11. J.D. Achenbach, in Mechanics Today (ed. S. Nemat-Nasser), p. 1, Pergamon Press, London, 1974.
12. B. Budiansky and R.J. O'Connell: Int. J. Solids and Structures, 1976, vol. 12, p. 81.
13. A. Vary, in Solid Mechanics Research for Quantitative Non-Destructive Evaluation (eds. J.D. Achenbach and Y. Rajapakse), p. 135, Kluwer Academic Publishers, Norwell, MA, 1987.
14. A.N. Sinclair, these Proceedings.
15. O. Buck, D.K. Rehbein and R.B. Thompson: Eng. Frac. Mech., 1987, vol. 128, No. 4, p. 413.
16. J.M. Coffey, in Mathematical Modelling in Non-Destructive Testing (eds. M. Blakemore and G.A. Georgiou), p. 7, Clarendon Press, Oxford, 1988.
17. J.D. Achenbach, A.K. Gautesen and H. McMaken: Ray Methods for Waves in Elastic Solids, p. 38, Pitman, Boston, 1982.
18. J.E. Gubernatis and E. Domany: J. Appl. Phys., 1979, vol. 50, p. 818.
19. W.M. Visscher: J. Appl. Phys., vol. 57, p. 1538.
20. J.L. Opsal and W.M. Visscher: J. Appl. Phys., 1985, vol. 58, p. 1102.
21. C.L. Scandrett and J.D. Achenbach: Wave Motion, 1987, vol. 9, p. 171.
22. C.L. Scandrett and G.A. Kriegsmann: Siam J. Sci. Stat. Comp., 1986, vol. 7, p. 571.
23. C.L. Scandrett, G.A. Kriegmann and J.D. Achenbach: J. of Comp. Physics, 1986, vol. 65, p. 1209.
24. L.J. Bond, in Research Techniques in NDT (ed. R.S. Sharpe), vol. 6, p. 107, Academic Press, New York, 1982.
25. K. Harumi: NDT International, 1986, vol. 19, no. 5, p. 315.
26. A.K. Mal: Q. Appl. Math., 1968, vol. 26, p. 231.
27. P.A. Martin, Proc. R. Soc. Lond., 1982, vol. A378, p. 262.

28. P.A. Martin and G.R. Wickam, Proc. Roy. Soc. London, 1983, vol. A390, p. 91.
29. W. Lin and L.M. Keer: Proc. Roy. Soc. London, 1986, vol. A408, p. 277.
30. W. Lin and L.M. Keer: J. Acoust. Soc. Am., 1987, vol. 82, p. 1442.
31. D. E. Budreck and J.D. Achenbach: J. Appl. Mech., 1988, vol. 55, p. 405.
32. D.A. Mendelsohn, J.D. Achenbach and L.M. Keer: Wave Motion, 1980, vol. 2, p. 277.
33. J.D. Achenbach and R.J. Brind, J. of Sound and Vibrations, 1981, vol. 76, p. 43.
34. R.J. Brind and J.D. Achenbach, J. of Sound and Vibrations, 1981, vol. 78, p. 555.
35. J.D. Achenbach, W. Lin and L.M. Keer, IEEE Trans. Sonics and Ultrasonics, 1983, vol. SU30, no. 4, p. 270.
36. A.H. Shah, Y.F. Chin and S.K. Datta, J. Appl. Mech., 1987, vol. 54, p. 761.
37. Ch. Zhang and J.D. Achenbach: Ultrasonics, 1988, vol. 26, p. 132.
38. Ch. Zhang and J.D. Achenbach: Wave Motion, 1988, vol. 10, in press.
39. Y.C. Angel and J.D. Achenbach: J. Acoust. Soc. Am. 1984, vol. 75, p. 313.
40. D.E. Budreck and J.D. Achenbach: J. Acoust. Soc. Am., submitted.
41. C.H. Yew, K.G. Chen and D.L. Wang, J. Acoust. Soc. Am., 1984, vol. 75, p. 189.
42. R. Dong and L. Adler: J. Acoust. Soc. Am., 1984, vol. 76, p. 1761.
43. B.Q. Vu and V.K. Kinra: J. Acoust. Soc. Am., 1985, vol. 77, p. 1425.
44. B.T. Khuri-Yakub, Y. Shui, G. Kino, D.B. Marshall and A.G. Evans, in Review of Progress in Quantitative Nondestructive Evaluation, Vol. 3, (D.O. Thompson and D.E. Chimenti, eds), Plenum Press, New York, 1984, p. 229.
45. S. Hirose and J.D. Achenbach, Int. J. for Num. Meth. in Eng., submitted.
46. N. Nishimura, Q.C. Guo and S. Kobayashi, in Boundary Elements IX, vol. 2 Stress Analysis Applications (eds. C.A. Brebbia, W.L. Wendland and G. Kuhn, p. 279, Springer-Verlag, Berlin, 1987.
47. J.D. Achenbach, W. Lin and L.M. Keer: 1986, Ultrasonics, vol. 24, p. 207.
48. J.D. Achenbach, D.A. Sotiropoulos and H. Zhu: J. Appl. Mech., 1987, Vol. 54, p.754.
49. P.A. Doyle and C.M. Scala: Ultrasonics, 1978, vol. 16, no, 4, p. 164.
50. M.G. Silk and B.H. Lidington: Brit. J. of NDT, 1975, vol. 17, no. 2, p. 33.
51. Y. Ogura: The Non Destructive Testing Journal of Japan, 1983, vol. 1, no. 1, p. 22.
52. K. Date, H. Shimada and N. Ikenaga: NDT International, 1982, vol. 15, p. 315.
53. J.D. Achenbach, L. Adler, D.K. Lewis and H. McMaken: J. Acoust. Soc. Am., 1979, vol. 66, p. 1848.
54. A.N. Norris and J.D. Achenbach: J. Acoust. Soc. Am., 1982, vol. 72, p. 264.
55. A.N. Norris: J. Acoust. Soc. Am., 1983, vol. 73, p. 421.
56. J.D. Achenbach, A.N. Norris, L. Ahlberg and B.R. Tittmann, in Review of Progress in Quantitative Nondestructive Evaluation, Vol. 2A, (eds. D.O. Thompson and D.E. Chimenti), p. 1097, Plenum, New York, 1982.

57. M. Kitahara, K. Nakagawa and J.D. Achenbach: Computational Mech., to appear.
58. A.K. Mal and L. Knopoff: J. Inst. Math. Its Appl., 1967, vol. 3, p. 376.
59. Ch. Zhang and J.D. Achenbach: J. Appl. Mech., 1988, vol. p.
60. J.E. Gubernatis, E. Domany, J.A. Krumhansl, and M. Huberman: J. Appl. Phys., 1977, vol. 48, p. 2812.
61. J.D. Achenbach, Ch. Zhang and D.A. Sotiropoulos, Metallurgical Trans., 1988, in press.
62. R.B. Thompson. O. Buck and D.K. Rehbein, in Solid Mechanics Research for Quantitative Nondestructive Evaluation (eds. J.D. Achenbach and Y. Rajapakse), p. 121, Kluwer Academic Publishers, Norwel, MA, 1987.
63. J.D. Achenbach and A.N. Norris: J. Nondestructive Eval., 1982, vol. 3, p. 229.
64. R.B. Thompson, L. Van Wyk, D.K. Rehbein, Y.-M. Tsai and O. Buck, these proceedings.
65. O. Buck, R.B. Thompson, D.K. Rehbein, L.J.H. Brasche and D.D. Palmer, these proceedings.